

WELDABILITY OF HIGHER NIOBIUM X80 PIPELINE STEEL

Chengjia Shang¹, Xiaoxiang Wang², Qingyou Liu³, Junyan Fu⁴

¹University of Science and Technology Beijing;

²Bohai Petroleum Equipment Co. Ltd.;

³Central Iron and Steel Research Institute;

⁴Microalloying Technology Center, CITIC Metals Co. Ltd.

Keywords: X80 Linepipe, Higher Niobium, Weldability, Toughness, HAZ

Abstract

Low carbon higher niobium-bearing microalloying design has been applied to develop X80 pipeline steel which can meet the requirement of the second west-east pipeline project (2nd WEPP). Since the beginning of application of X80 hot strip and plate steel, weldability of this steel has been paid serious attention. Results from recent simulation researches show that the optimum heat input energy for Nb-bearing X80 steel should be lower than 30 kJ/cm. Characterization of the CGHAZ in the actual welding sample of the higher Nb-bearing steel shows that the size of Nb(CN) precipitates does not coarsen obviously compared to the normal precipitates (≤ 30 nm) in the X80 pipeline steel with conventional Nb content. Furthermore, the prior austenite grain size in the HAZ of 0.09%Nb steel is smaller than in 0.06%Nb steel. The industrial DSAW results show that the higher Nb (0.09%) X80 steel can be successfully, more efficiently welded to get good performance. Many industrial testing results show that with appropriate welding processing control, the mechanical properties of the HAZ in higher Nb X80 steel, especially the toughness, could reach high levels. That promises a great insurance for the success of the construction of the 2nd WEPP.

Introduction

The development of X80 pipeline steel was started in 2003 in China. The demonstration section of 7.9 km long, 1066 mm diameter X80 pipeline was constructed in 2005. From 2006, the second west-east pipeline project was designed and started. So far the Chinese steel and pipe mills have made several trials to develop X80 strip/plate steel and spiral/longitudinal submerged arc welded pipe.

The Second West-East Pipeline Project is the initial pipeline project which transports natural gas from a foreign country to China. Natural gas from Turkmenistan is transported through the Central Asian Natural Gas Pipeline to Horgos in Xinjiang Province, and then through the 2nd WEPP to the Guangzhou Province of South China. The transport capacity of the 2nd WEPP is 30 billion m³/a. The length of the mainline is 4895 km, and the diameter of the pipe is 1219 mm with 18.4/22/26.4/27.5 mm wall thickness. Transport pressure is 12 MPa in the west section and 10 MPa in the east section. The X80 pipeline steel is employed in the trunk line with a total amount of more than 4,000,000 tonnes. The west section has already been put into application in September 2009, while the east section has been completed successfully in June 2011.

The low carbon higher niobium alloy design was firstly employed in X80 pipeline steel in North American pipeline projects [1]. The higher Nb content X80 steel shows a good strength/toughness balance and the alloy cost is lower. At the beginning of drawing up the standards for X80 pipeline steel for the 2nd WEPP, the international specification rules (API 5L and ISO 3183), in which the limitation of niobium addition is 0.06 wt%, were considered. However, due to the demonstration of the North American application and some prior research results from overseas [2], the new concept that the content of niobium could exceed 0.06% at low carbon content was accepted by the Chinese pipeline industry and Chinese metallurgy community [3, 4]. The upper limit of niobium content was modified to 0.11%, while the total content of Nb+V+Ti is not allowed higher than 0.15%. In the results from Chinese steel mill trials and physical metallurgy research [5-9], it is shown that the higher Nb X80 is capable of meeting the requirement of X80 pipeline specification. Furthermore, results from both laboratory research on weldability of higher Nb content steel [10] and industrial trials were carried out to reveal the relationship between welding process parameters, microstructure and mechanical properties in the HAZ. In this paper, results from the research on weldability of higher Nb X80 steel will be introduced, and the large amount of X80 linepipe testing data will be reported.

Thermo-Simulation Study of Weldability of X80

With the HTP microalloying approach route of low carbon high Mn and high Nb, the trials on X80 pipeline strip and plate steel have been carried out in industry from 2007, in which the Nb content is about 0.10%, and the total Ti+V+Nb is less than 0.15%. The results from this preliminary stage show that low carbon high niobium without molybdenum design can reach the strength and toughness level of X80 longitudinal submerged arc welded pipe, and with 0.2-0.3% molybdenum addition, it can meet the strength and toughness requirement of X80 spiral submerged arc welded pipe.

In the first stage of developing X80 pipeline steel for 2nd WEPP, it was suspected that a higher niobium content could cause coarse precipitates which could be detrimental to HAZ toughness. Therefore, a research project was carried out to focus on the weldability of higher niobium X80 pipeline steel made up of both pipe mills and research institutes. This project helped the successful manufacture of large scale production X80 pipes for 2nd WEPP. Meanwhile, a large amount of data has been obtained and improved the understanding of relationships between composition, process, microstructure and properties, as well as promoting the progress of niobium microalloyed pipeline steel making technology.

In order to study the weldability of low C high Mn high Nb steel and the reason for toughness decreasing in the CGHAZ, thermal simulation of single pass CGHAZ was performed on a Gleeble-1500 [10]. This was based on 6 heat inputs (16, 20, 30, 40, 50, 58 kJ/cm) from actual welding parameters. The thermal cycle simulations are shown in Figure 1.

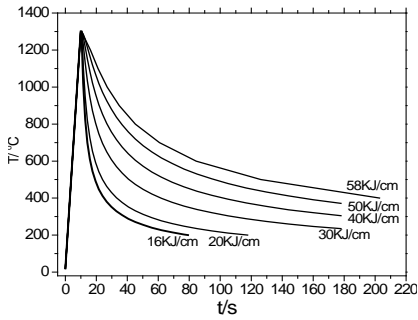


Figure 1. Thermal cycle curves under different heat input values.

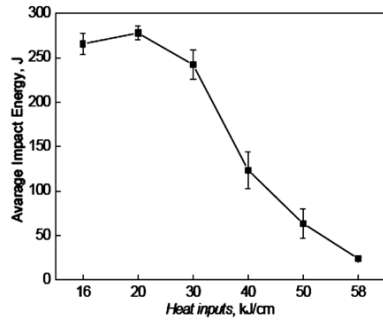


Figure 2. Impact energy under different heat input conditions (-20 °C).

After welding thermal cycle simulation, the -20 °C Charpy impact energy of the thermal simulation specimens under different heat input values was determined. The impact toughness data are shown in Figure 2. Under low heat input (16 kJ/cm - 30 kJ/cm), the toughness of the CGHAZ is better. Impact toughness decreases substantially with the increasing heat input, from 40 kJ/cm to 60 kJ/cm.

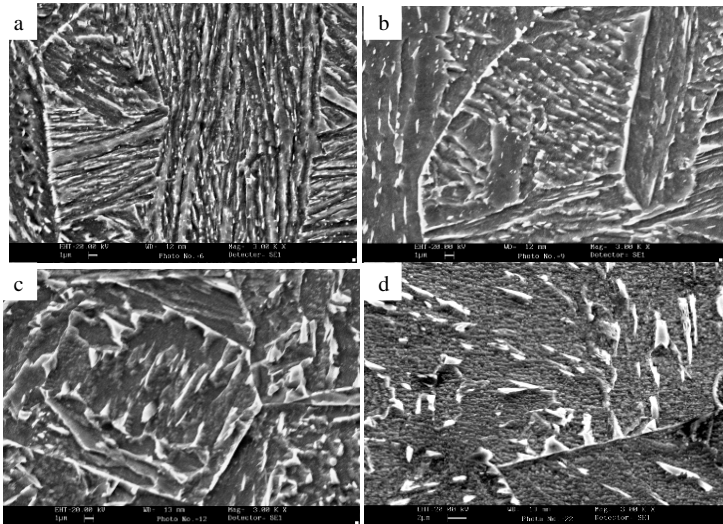


Figure 3. Microstructures of CGHAZ under different heat inputs, (a) 20 kJ/cm ($t_{8/5} = 9.5$ s), (b) 30 kJ/cm, (c) 40 kJ/cm, (d) 58 kJ/cm ($t_{8/5} = 80.9$ s).

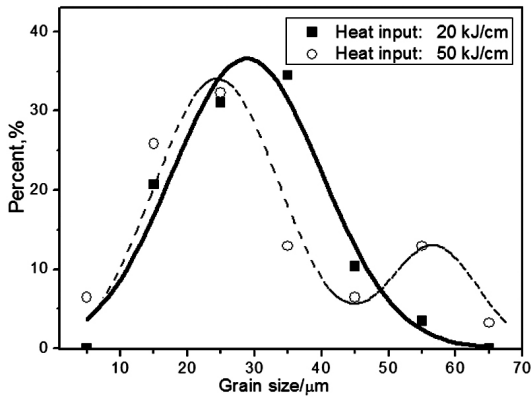


Figure 4. Size distributions of prior austenite grains in CGHAZ of higher Nb X80 steel under different heat inputs.

SEM photographs of microstructure are shown in Figure 3. The distribution and size of MA product under different heat inputs can be seen clearly. MA is the white highlighted particles, distinguished from the grain boundary. Under low heat inputs (16 kJ/cm – 30 kJ/cm), MA is fine and well aligned. With increasing heat input, MA is coarsening and the size is larger than 2 μm .

The size distribution of prior austenite grains in the CGHAZ is shown in Figure 4. High heat input significantly increased the portion of large size austenite grains, and the uniformity of prior austenite grains in CGHAZ was seriously deteriorated.

Figure 5 shows the EBSD results of Kikuchi band contrast maps from the specimens under different heat inputs. White lines represent the grain boundaries with misorientation above 15° . As shown in Figure 5, the microstructure mainly consists of lath bainite under low heat input, Figure 5(a), and granular bainite under high heat input, Figure 5(b). When the heat input is low, the grain size of prior austenite is small, adjacent laths within a packet [11] exhibit low misorientation (low angle boundaries). High angle boundaries always occur where packets meet. Thus effective grain size is the size of the packets within prior austenite grains. However, when the heat input is high, granular bainite is mainly obtained; bainitic ferrites in the granular bainite have similar orientation. That makes the density of high angle boundary in the prior austenite pretty low. In this case the effective grain size should be considered as the size of the coarse prior austenite grains. The white constituents in Figure 5(a) and 5(b) are fcc phase identified by EBSD. Under high heat input, the size of residual austenite particles is quite large. In addition to the high angle boundaries within prior austenite grains, prior austenite grain boundaries are another significant provider of high angle boundaries. Small prior austenite grains have a high density of high angle grain boundary. Lath bainite formed during continuous cooling inside the austenite grains also exhibits a high density of high angle grain boundary. High angle boundaries effectively inhibit the nucleation and propagation of brittle cracks [12-14], and improve the fracture resistance further.

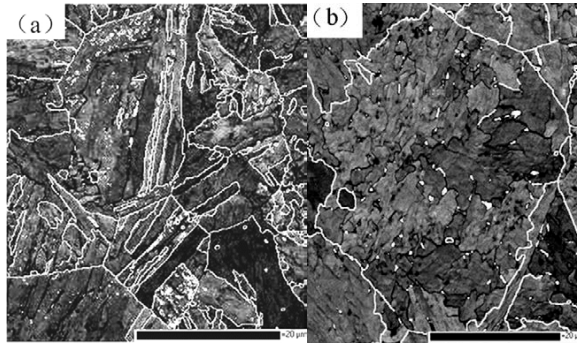


Figure 5. Band contrast maps under different heat inputs (white lines are high angle boundaries with misorientation $\geq 15^\circ$) (a) 20 kJ/cm ($t_{8/5} = 9.5$ s), (b) 50 kJ/cm ($t_{8/5} = 58.7$ s).

There is no doubt that the size and uniformity of prior austenite grains have a significant impact on the toughness of the CGHAZ. Transformation product is another main factor which can influence the toughness of the CGHAZ. Solute niobium and precipitated niobium particles influence not only the coarsening of prior austenite grains but also the phase transformation mechanism during the welding thermal cycle. The microstructure in the CGHAZ is obtained as follows: the base metal is reheated to fully austenite, and then continuously cooled without deformation. Higher niobium bearing steel has an obvious advantage of suppressing the coarsening of prior austenite grains and keeping the uniformity of grains, both of which are beneficial to the following phase transformation. Higher niobium content is also favorable to the formation of middle and low temperature transformation microstructure [12], which ensures the HAZ structure and base metal have good matching. Control of heat input is still the main way to improve the toughness of the CGHAZ. Too high heat input could cause the coarsening of prior austenite grains in CGHAZ, making the final transformation product coarse, with a low density of high angle boundaries in granular bainite, and leave the MA product as massive blocks [15, 16]. Such a microstructure with a sharp reduction of high angle boundaries and coarse MA is strongly detrimental to toughness.

Actual Welding Process, Microstructure and Properties

Welding Processes

Spiral (Helical) and longitudinal pipe submerged arc welding processes (SAWH and SAWL) are described as below:

SAWH tubes: outer diameter 1219 mm, wall thickness 15.3/18.4 mm, and the pipes, formed by the process of uncoiling, flattening, three-roll shaping, were welded by double-sided submerged arc welding. Consumables used were Mn-Mo-Ti-B welding wire and fluoride alkali high toughness sintered flux.

SAWL tubes: outer diameter 1219 mm, wall thickness 22/26.4/27.5 mm, formed by the process of JCO or UO, were continuously pre-welded, and then welded by double-sided submerged arc

welding. The inside welding employed four wire tandem submerged arc welding, while the outside welding adopted four or five wire tandem submerged arc welding. Consumables used were Mn-Mo-Ti-B welding wire and fluoride alkali high toughness sintered flux same as for SAWH. The tubes were mechanically expanded after welding.

According to the results of thermal simulations above, the heat input was controlled to make sure it did not exceed 30 kJ/cm.

Welding Physical Metallurgy

Generally, the grain size in the HAZ will seriously coarsen near the fusion line, and the subsequent transformed microstructure will be much larger. However, TiN plays a key role to resist the grain growth and guarantee better toughness in the HAZ. Therefore the best Ti/N ratio should be employed in pipeline steel. Since the N content can be usually controlled to less than 60 ppm in the steel making process, the addition of Ti should be optimized to control the Ti/N ratio. Several researches of actual welding HAZ show that the Ti/N ratio is usually in the range from 2.0 to 3.5 for industrially manufactured steels, the toughness of the HAZ is fine and in this range there is no significant evidence showing that the Ti/N ratio affects grain size and microstructure in the HAZ. It can be concluded that Ti addition should be in the range from 0.01% to 0.02%.

For double-side welding or multiple pass welding, the HAZ of the first pass and the second pass is overlapped, as shown in Figure 6. CGHAZ and ICCGHAZ are the least tough areas of welding HAZ. Samples prepared to make extraction replica samples for the observation by TEM were cut from the CGHAZ and ICCGHAZ of industrial steel No.1 and No. 2 (chemical composition is listed in Table I, in which steel No. 1 contains medium niobium while No. 2 contains higher niobium). TEM observation showed the precipitation of niobium in the industrial higher and medium niobium bearing pipeline steel. In addition, the status of prior austenite grains in the HAZ with different niobium content was also studied.

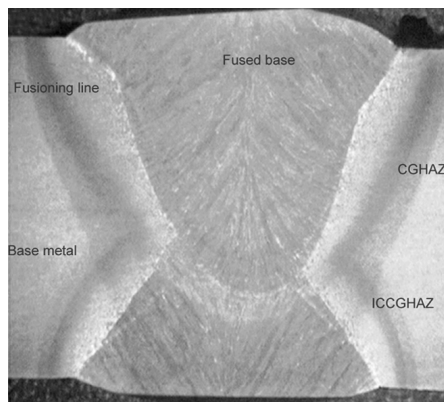


Figure 6. Actual welding heat affected zone.

Table I. Chemical Compositions of the Experimental X80 Pipeline Steels (wt %)

No.	C	Si	Mn	Nb	Mo	Cr + Cu + Ni and others
1	0.08	0.17	1.64	0.05	0.21	≥ 0.50
2	0.06	0.18	1.79	0.09	0.24	≥ 0.50

Observations of precipitation in the CGHAZ and ICCGAZ of medium and higher niobium bearing steel welding specimens are shown in Figure 7 and Figure 8 respectively, including TEM photographs and energy spectrum results of the precipitated particles. The precipitates from the two low-toughness areas of the two steels with different Nb content are almost elliptical particles. Energy spectrum analysis shows that the particles are mainly precipitates of niobium.

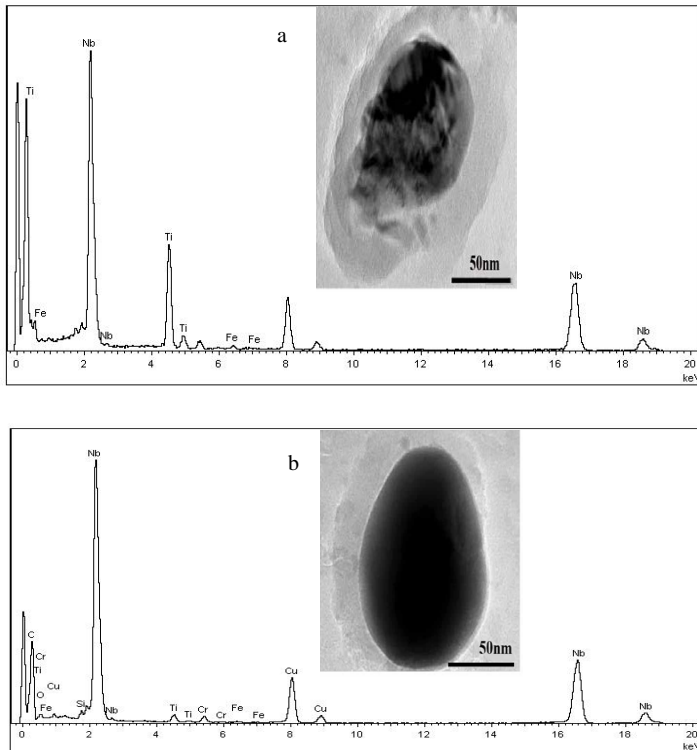


Figure 7. Precipitated particles in HAZ of Medium Nb steel (No. 1): (a) Precipitate particle in CGHAZ and its energy spectrum analysis, (b) precipitate particle in ICCGAZ and its energy spectrum analysis.

Size distributions of precipitates in different areas of steel No.1 (0.05%Nb) and steel No.2 (0.09%Nb) HAZ are shown in Figure 9. Simulated CGHAZ from single pass welding is characterized. As shown in Figure 9(a), the precipitates in the CGHAZ of medium niobium steel have small size less than 20 nm, while the size of precipitates from higher niobium steel is almost 40~50 nm. Extremely large precipitates are not detected in either steel. These fine particles are beneficial to prevent grains from coarsening in both cases.

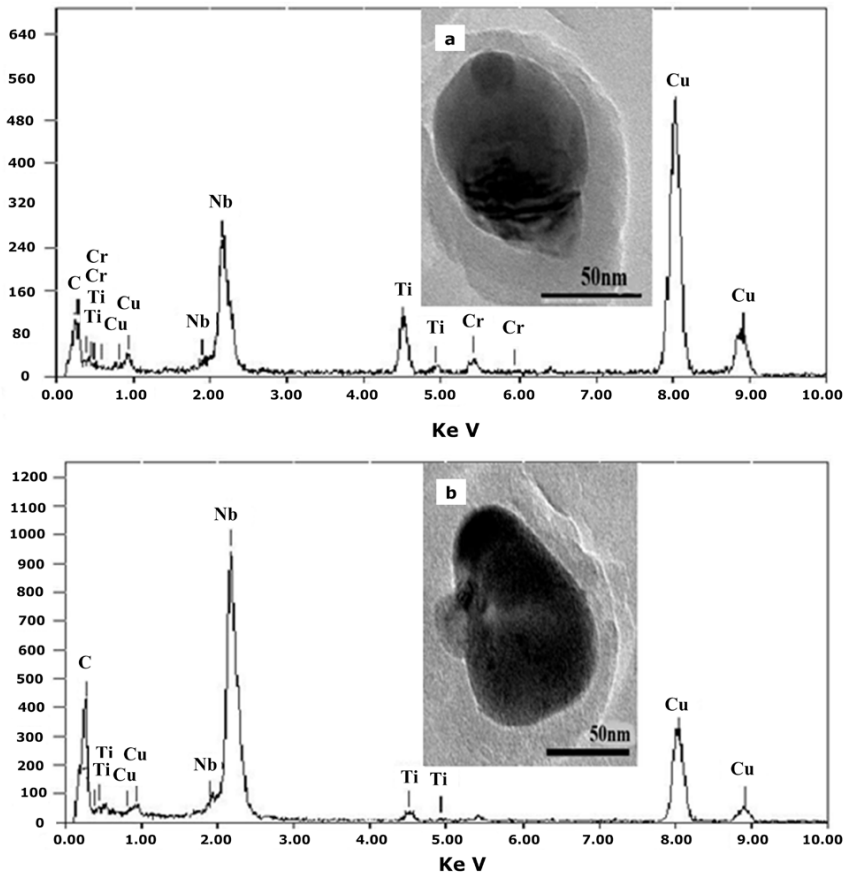


Figure 8. Precipitated particles in HAZ of Higher Nb steel (No. 2): (a) precipitate particle in CGHAZ and its energy spectrum analysis, (b) precipitate particle in ICCGAZ and its energy spectrum analysis.

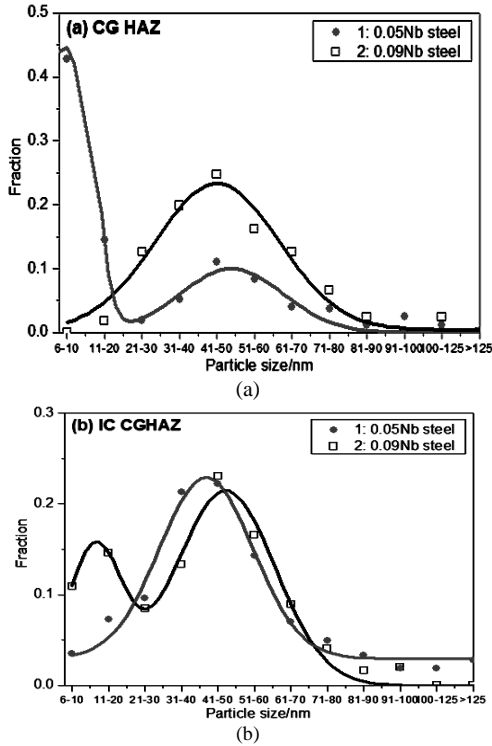


Figure 9. Size distributions of precipitated particles in HAZ of different Nb steels: (a) CGHAZ; (b) ICCGAZ.

In order to study the nature of prior austenite in the whole HAZ, the prior austenite grain boundaries were investigated, Figure 10. Prior austenite grain size coarsened a lot in the HAZ. The most serious coarsening happened in the region close to the fusion line. With the increase of distance from the fusion line, the size of prior austenite grains decreased gradually. The distributions of CGHAZ in medium and higher niobium bearing steel, respectively, are marked in Figure 10(a) and Figure 10(b) respectively. The width of the CGHAZ in steel No.1 (0.05%Nb) is about 225 μm , while the width of the CGHAZ in steel No.2 is less than 200 μm . Prior austenite grains in the HAZ of steel No.1 coarsened more seriously than in steel No.2. Different niobium content is likely to be the main reason which caused the difference in CGHAZ between the two samples. Higher niobium content retards the grain boundary mobility [10,11] and thus suppress austenite grain coarsening. Also, fine niobium precipitates pin the grain boundaries and inhibit the growth of austenite grains.

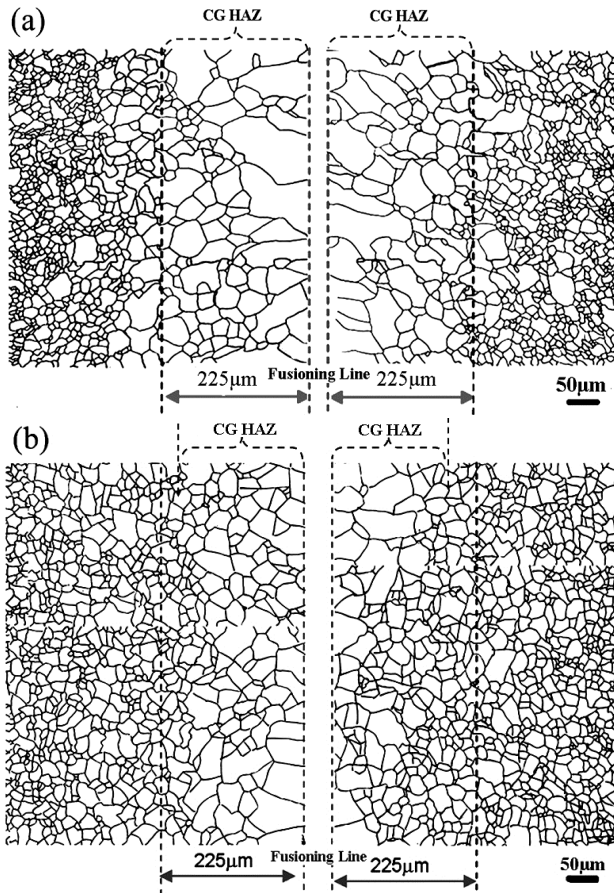


Figure 10. Distribution of prior austenite grains in the HAZ (a) medium Nb steel (0.05wt%); (b) higher Nb steel (0.09wt%).

Mechanical Properties of Spiral Submerged Arc Welded Pipe

Table II shows the chemical composition of X80 hot strip spiral pipe. Clearly the higher Nb design was applied.

Table II. Typical Composition of X80 Hot Strip Steel for 2nd WEPP

	C	Mn	Si	P	S	Nb	V	Ti	Mo	Ni	Cr	Cu	Nb+ V+Ti
Max.	0.06	1.88	0.24	0.01	0.002	0.10	0.02	0.02	0.27	0.26	0.25	0.25	0.13
Min.	0.03	1.76	0.16	0.01	0.001	0.06	0.01	0.01	0.21	0.21	0.01	0.02	0.10
Ave.	0.05	1.83	0.19	0.01	0.001	0.08	0.02	0.01	0.24	0.25	0.02	0.22	0.11

Statistical results of tensile tests from 1455 heats of spiral welded pipe for 2nd WEPP are shown in Table III. Production test data of strip steel from 4 mills (A, B, C, D) is included. All the data meets the required specification. The average yield ratio is about 0.86.

The statistical results of Charpy impact tests at -10 °C from 1297 heats of spiral welded pipe body are shown in Table IV, while weld seam test results are shown in Table V, and HAZ test results are shown in Table VI. Manufacturers' test data of plate coil for making tubes from 4 mills (A, B, C, D) was included. The average Charpy impact energy of the pipe body was about 350 J, and all the average shear areas were 100%. The Charpy energy of the pipe body and plate coil were similar. The average Charpy impact energy of the weld seam was about 160 J. The average Charpy impact energy of the HAZ was about 200 J. All Charpy energies are above the specified minima. That shows a combination of excellent impact toughness and welding performance of low carbon high niobium steel. Charpy impact energy histograms of pipe body, weld seam and HAZ of X80 plate coil from D mill are shown in Figure 11. The results match the normal distribution and indicate a good toughness control.

Table III. Tensile Test Data of Spiral Pipes Made of Hot Strip Steels Supplied by 4 Mills (A, B, C, D)

Project		Tensile Strength Rm (MPa)	Yield Strength Rt0.5 (MPa)	Elongation (%)	Yield Ratio
A (229 sets)	Min.	651	555	21.5	0.73
	Max.	789	652	29.6	0.91
	Ave.	708	581	25.4	0.82
B (46 sets)	Min.	672	555	22.4	0.74
	Max.	759	612	29	0.89
	Ave.	706	572	25.8	0.81
C (799 sets)	Min.	647	555	19.6	0.75
	Max.	794	684	30	0.94
	Ave.	698	592	25	0.85
D (381 sets)	Min.	643	555	21.4	0.75
	Max.	780	686	29.5	0.93
	Ave.	691	593	25.0	0.86
Specification		625~825	555~690	≥16	≤0.94
Average Difference of Tubes and Plates		+2	+23	-1	+0.03

Table IV. Charpy Impact Test Data of Pipe Body Made of Hot Strip Steels Supplied by 4 Mills (A, B, C, D)

Testing Temperature (-10 °C)	Impact Energy (J)			Shear Area (%)		
	Min.	Max.	Ave.	Min.	Max.	Ave.
A (192 sets)	262	464	352	96	100	100
B (41 sets)	272	441	353	100	100	100
C (715 sets)	251	497	352	86	100	100
D (349 sets)	215	477	343	83	100	100
Specification	Single ≥ 170 J, Average ≥ 220 J			Single ≥ 80 %, Average ≥ 90 %		
Average Difference of Tubes and Plates	+5			+1		

Table V. Charpy Impact Test Data of Weld Seam, with Steels Supplied by 4 Mills (A, B, C, D)

Testing Temperature (-10 °C)	Impact Energy (J)			Shear Area (%)		
	Min.	Max.	Ave.	Min.	Max.	Ave.
A (192 sets)	61	221	162	37	100	70
B (41 sets)	82	221	166	42	98	71
C (715 sets)	66	241	167	38	100	72
D (349 sets)	72	265	158	41	100	68
Specification	Single \geq 60 J, Average \geq 80 J			Single \geq 30%, Average \geq 40%		

Table VI. Charpy Impact Test Data of HAZ, with Steels Supplied by 4 Mills (A, B, C, D)

Testing Temperature (-10 °C)	Impact Energy (J)			Shear Area (%)		
	Min.	Max.	Ave.	Min.	Max.	Ave.
A (192 sets)	90	291	205	42	100	90
B (41 sets)	73	285	211	43	100	91
C (715 sets)	62	295	206	38	100	90
D (349 sets)	62	296	199	41	100	96
Criteria Requirement	Single \geq 60J, Average \geq 80J			Single \geq 30%, Average \geq 40%		

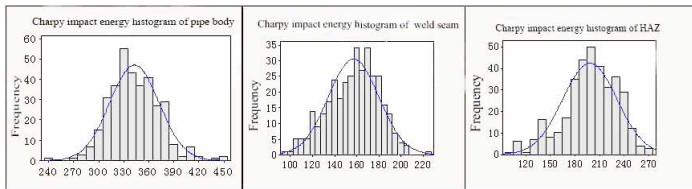


Figure 11. Charpy impact energy histogram of pipe body, weld seam and HAZ of X80 plate coil from D mill (Energy in J).

The statistical results of DWTT tests from 1561 heats of spiral welded pipe body are shown in Table VII. The DWTT results of the X80 tubes made from hot strip steel from 4 mills are acceptable. Average shear areas are almost 100%.

Table VII. Statistical Results of DWTT Test of Spiral Welded Pipe Body

Group	SA%	1	2	Average
A (192 sets)	Min.	78	92	89
	Max.	100	100	100
	Ave.	100	100	100
B (304 sets)	Min.	92	94	93
	Max.	100	100	100
	Ave.	100	100	100
C (716 sets)	Min.	96	92	94
	Max.	100	100	100
	Ave.	100	100	100
D (349 sets)	Min.	100	100	100
	Max.	100	100	100
	Ave.	100	100	100

Table VIII. Statistical Results of HV10 Hardness Test of Spiral Welded Pipe Body

HV10	Max.	Min.	Ave.
A (192 sets)	268	191	228
B (41 sets)	248	198	227
C (715 sets)	270	176	228
D (349 sets)	258	180	225

The statistical results of HV10 hardness tests from 1297 heats of spiral welded pipe body are shown in Table VIII. The average value of hardness doesn't exceed 230 HV10, and the highest value of hardness is 270 HV10 which is below the maximum value of 280 HV10 provided by the specification.

All the data above show that the spiral welded X80 pipe for 2nd WEPP has excellent mechanical properties.

Mechanical Properties of Longitudinal Submerged Arc Welded Tubes

The chemical composition of X80 plate steel for 2nd WEPP is shown in Table IX. It can be seen that there were 2 kinds of chemical composition of X80 plates: Nb+Cr and Nb+Cr+Mo. The carbon content of X80 plate steel is very low: 0.04%-0.06%. Compared with X70 developed before, X80 has higher Mn and Nb content and lower Mo content, and that reduced the cost.

Table IX. Chemical Composition of X80 Plate Steel for 2nd WEPP

No.	C	Mn	Si	P	S	Nb	V	Ti	Mo	Ni	Cr	Cu	Nb+V+Ti
1	0.06	1.86	0.26	0.008	0.003	0.053	0.024	0.016	0.250	0.244	0.210	0.130	0.093
2	0.06	1.71	0.20	0.005	0.003	0.088	0.002	0.010	0.001	0.176	0.294	0.196	0.100
3	0.04	1.70	0.27	0.008	0.003	0.100	0.002	0.018	0.006	0.009	0.243	0.235	0.120

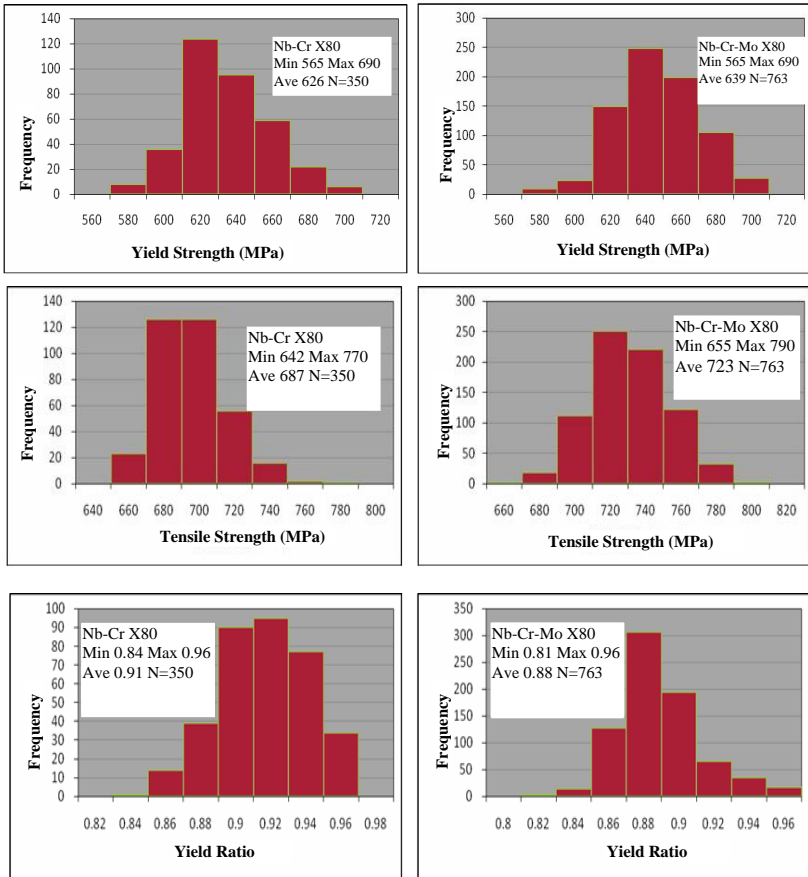


Figure 12. Comparison of tensile strength of Nb-Cr and Nb-Cr-Mo X80 tubes.

The yield strength, tensile strength and yield ratio of Nb-Cr and Nb-Cr-Mo X80 tubes are shown in Figure 12. It shows that average yield strength of Nb-Cr-Mo X80 tubes is larger than Nb-Cr

X80 tubes by 13 MPa, and average tensile strength is higher by 36 MPa. The yield ratio of Nb-Cr-Mo X80 tubes is mostly below 0.92, with only a few tubes with a yield ratio of 0.94 or 0.96.

The Charpy energy of Nb-Cr and Nb-Cr-Mo X80 tubes' body, weld seam and HAZ are shown in Figure 13. The value and distribution of Charpy energies of the two JCOE tube bodies are quite different. The Charpy energy of Nb-Cr X80 tubes body is much higher than Nb-Cr-Mo tubes, but two peaks were detected in Nb-Cr X80 tubes as the statistical results come from different suppliers and/or different stages (dates). The Charpy energies of the two JCOE tubes weld seams are almost the same. The higher Charpy energy samples of Nb-Cr X80 HAZ might be related to the higher Charpy energy of the base metal.

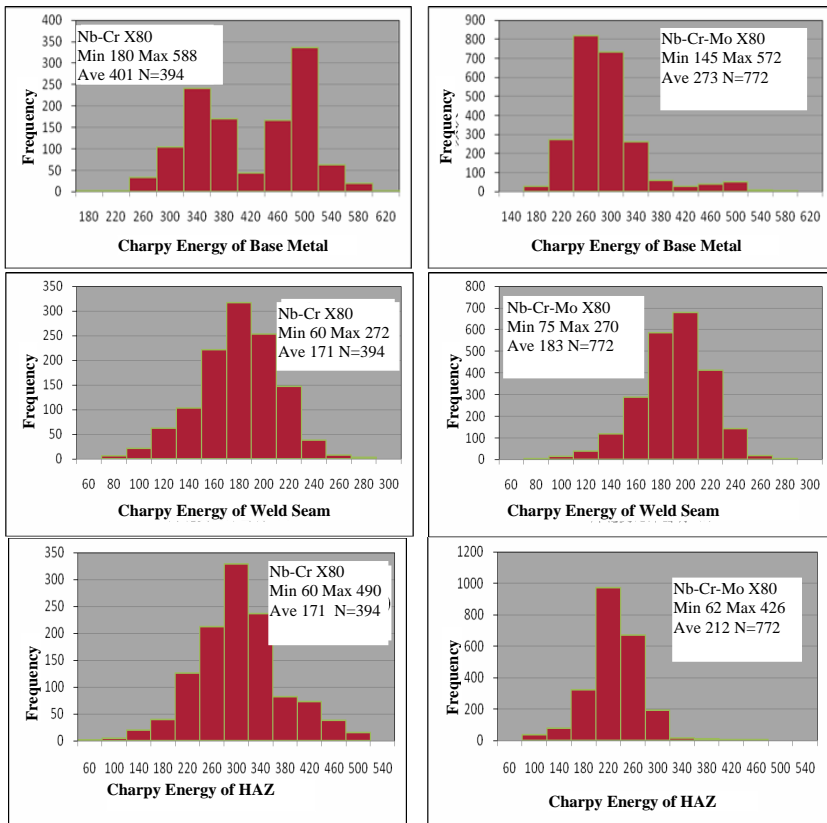


Figure 13. Comparison of Charpy impact toughness of Nb-Cr and Nb-Cr-Mo X80 tubes' body, weld seam and HAZ, energy in J.

The statistical data of DWTT properties of Nb-Cr and Nb-Cr-Mo X80 tube bodies are shown in Figure 14. The DWTT average shear area of Nb-Cr X80 tube is slightly higher than Nb-Cr-Mo X80 tube, but the frequency of higher and lower value is higher. The reason might be that at the trial stage of producing Nb-Cr pipeline steel, the DWTT property was not tightly controlled. With the optimization of TMCP technology, the DWTT of higher Nb-bearing X80 pipeline steel was improved a lot. In addition, DWTT shear area of X80 SAWL pipe is lower than spiral welded pipe. This may be related to the thickness of the wall. The wall of spiral welded pipe is thinner which may benefit the DWTT property.

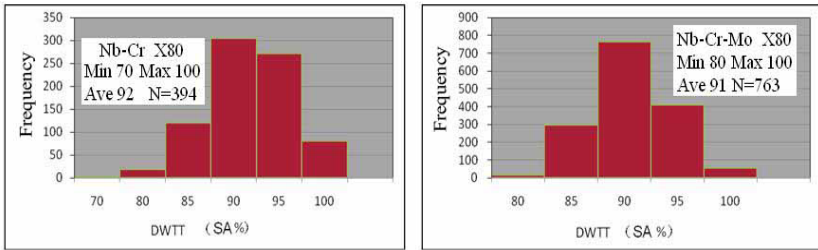


Figure 14. Comparison of DWTT property data of Nb-Cr and Nb-Cr-Mo X80 tube bodies.

Summary

According to the weldability research results of low carbon higher niobium X80 steel, the optimum heat input energy should be lower than 30 kJ/cm. The distribution and size of MA constituent are mostly influenced by cooling rate between T_{8/5} and can be addressed by control of welding parameters. No evidence has been found that coarse niobium precipitates have an effect on the properties in the CGHAZ and ICCGHAZ by TEM investigation in actual welding samples. By comparing the 0.06% Nb content and the 0.09% Nb content in actual X80 welding samples, it shows that the grain size in the CGHAZ of higher Nb steel is much finer than in the 0.06% Nb-bearing X80 pipeline steel.

The development of low carbon higher niobium X80 pipeline steel contributed greatly to the success of the manufacture of X80 pipe for 2nd WEPP. Statistical analysis showed that those pipes have good mechanical properties, especially the toughness. Excellent weldability is achieved and ensures the successful progress of the project.

Some issues still need further investigation. For example, transverse yield ratio is a little bit higher especially after strain aging. Therefore a pre-strain and aging resistance pipeline steel should be developed in future. The alloy design should be further modified to reduce the cost of X80 pipeline produced by some mills. Higher grade X90 and X100 need to be developed with the increasing transport capacity needed for future pipeline projects in China. The breakthrough improvement of Chinese pipeline technology is needed for the construction of the next round of pipeline projects.

Acknowledgments

The authors are grateful for the excellent work on the joint project and contributions for this paper to Mr. Yanhong Fu, Mr. Yanfen Li, Mr. Xiaowei Chen from Bohai Petroleum Equipment Co. Ltd., Ms. Shujun Jia, Mr. Bin Wang and Dr. Xinjun Sun from Central Iron and Steel Research Institute, Ms. Huoran Hou, Mr. Weizhe Wang from Microalloying Technology Center, CITIC Metals Co. Ltd., and Dr. Hui Guo, Prof. Xuemin Wang, Dr. Chengliang Miao, Mr. Zhenwei Liu, Mr. Xueda Li, Mr. Yang You from University of Science and Technology Beijing.

References

1. K. Hulka, P. Bordignon and J.M. Gray, "Niobium Technical Report-No 1/04, Companhia Brasileira de Metalurgia e Mineração (CBMM) 2004" (Paper presented at International Seminar the High Temperature Processing Steel Project, São Paulo, Brazil, 2003).
2. D.G. Stalheim, K.R. Barnes and D.B. McCutcheon, "Alloy Designs for High Strength Oil and Gas Transmission Linepipe Steels," *International Symposium of Microalloyed Steels for the Oil and Gas Industry*, Companhia Brasileira de Metalurgia e Mineração (CBMM) / The Minerals, Metals and Materials Society (TMS), Brazil, 2006.
3. The Technical Conditions of X70 LSAW Linepipe for the Second West to East Gas Pipeline Project. China Petroleum Enterprise Standardization, 2007 (in Chinese).
4. The Technical Conditions of the Hot Rolling Steel Plate for the Second West to East Gas Pipeline Project. China Petroleum Enterprise Standardization, 2007 (in Chinese).
5. C.L. Miao et al., "Grain Refinement and Microstructure Control of HTP X80 Pipeline Steel," *Iron and Steel*, 44 (3) (2009), 62-66 (in Chinese).
6. T.X. Cui et al., "Effect of the Composition and Process on Microstructure and Properties of X80 Pipeline Hot Strip," *Iron and Steel*, (2009), 44-55 (in Chinese).
7. C.L. Miao et al., "Recrystallization and Strain Accumulation Behaviors of High Nb-bearing Line Pipe Steel in Plate and Strip Rolling," *Materials Science and Engineering A*, 527 (2010), 4985.
8. C.L. Miao, G.D. Zhang and C.J. Shang, "Recrystallization and Strain Accumulation Behaviors of High Nb-bearing Line Pipe Steel in Plate and Strip Rolling," *Materials Science Forum*, 62 (2010), 654-656.
9. C.L. Miao et al., "Refinement of Prior Austenite Grain in Advanced Pipeline Steel," *Frontiers of Materials Science in China* 4, 197 (2010).
10. C.L. Miao et al., "Microstructure and Toughness of HAZ in X80 Pipeline Steel with High Nb Content," *Acta Metallurgical Sinica*, 46 (2010), 541-546 (in Chinese).

11. H. Kitahara et al., "Crystallographic Features of Lath Martensite in Low-Carbon Steel," *Acta Materialia*, 54 (2006), 1279–1288.
12. B. Hwang et al., "Effective Grain Size and Charpy Impact Properties of High-Toughness X70 Pipeline Steels," *Metallurgical and Materials Transactions A*, 36A (2005), 2107.
13. Y. Ohomori, H. Ohtani and T. Kunitake, "Tempering of the Bainite and the Bainite/Martensite Duplex Structure in a Low-Carbon Low-Alloy Steel," *Metal Science*, 8 (1974), 357–366.
14. J.P. Naylor and P.R. Krahe, "The Effect of the Bainite Packet Size on Toughness," *Metallurgical Transactions*, 5 (1974), 1699.
15. S. Lee, B.C. Kim and D.Y. Lee, "Fracture Mechanism in Coarse Grained HAZ of HSLA Steel Welds," *Scripta Metallurgica*, 23 (1989), 995.
16. Y. Li and T.N. Baker, "Effect of Morphology of Martensite-Austenite Phase on Fracture of Weld Heat Affected Zone in Vanadium and Niobium Microalloyed Steels," *Materials Science and Technology*, 26 (9) (2010), 1029-1040.